Light Scattering Study of Sodium Dodecyl Polyoxyethylene-2-sulfate Micelles in the Presence of Multivalent Counterions

R. Alargova, J. Petkov, D. Petsev,* I. B. Ivanov, G. Broze,† and A. Mehreteab‡

Laboratory of Thermodynamics and Physico-chemical Hydrodynamics, Faculty of Chemistry, Sofia University, 1126 Sofia, Bulgaria, Colgate-Palmolive Research and Development, Inc., Avenue Du Parc Industriel, B-4041 Milmort (Herstal) Belgium, and Colgate-Palmolive Company, Technology Center, 909 River Road, Piscataway, New Jersey 08854-5596

The properties of ionic micelles of sodium dodecyl polyoxyethylene-2-sulfate in the presence of multivalent ions were investigated by means of light scattering methods. It was shown that divalent and especially trivalent counterions may lead to dramatic change in the micellar size and shape even at very low ionic strength. This effect is particularly pronounced for trivalent counterions as Al^{3+}. The persistent lengths for some rod-shaped micelles were obtained and the energy of bending of such rods was estimated. The solubilization capacity of sodium dodecyl polyoxyethylene-2-sulfate was shown to be also dependent on the presence of divalent and trivalent ions. It increases with varying the counterion valence from one to three. The increase of the solubulization capacity of anionic surfactants in the presence of divalent and furthermore trivalent counterions could be of practical importance since it is directly related to the cleaning action of given detergent composition.

1. Introduction

It is well-known that surfactant molecules can organize themselves into aggregates when dissolved into water medium. Usually, they form spherical micelles when the concentration of monomers exceeds a certain value which defines the critical micellization concentration (cmc). However, in some cases it is possible to obtain other (higher order) aggregates such as cylindrical micelles, multilayer vesicles, etc.[1] The existence of such complex structures depends mainly on the surfactant structure and concentration, ionic strength of the solution, and temperature.[1-9] It was shown in these studies that above a given concentration of electrolyte in the solution the micellar aggregation number increases and the micellar shape transforms from spherical into cylindrical. The typical values of 1:1 electrolyte concentrations necessary to initiate such transition is relatively high, about 0.5–1 M and even higher.[2-9] All these studies were performed using *only* monovalent electrolyte. However, it is established that the specific type (i.e., the valence) of microions present may affect strongly the aggregation number of the micelles, although the cmc value depends mainly on the overall ionic strength.[9] This fact may be due to the stronger binding of multivalent counterions to the micellar surface, thus decreasing the repulsion between the polar head groups of the surfactant molecules and increasing the local curvature.

The aim of the present paper is to analyze the transition from spherical into cylindrical shape of anionic (sodium dodecyl polyoxyethylene-2-sulfate, SDP-2S) micelles in the presence of multivalent counterions. For that purpose we applied light-scattering methods which enabled us to obtain the geometrical properties of the micelles similar to previous studies.[2-9] We show that micelles in the presence of divalent and trivalent ions exhibit similar shape changes as in the presence of monovalent ones. However, an important difference is that in the case of multivalent counterions this transition takes place at ionic strengths about 1 order of magnitude lower than those when only monovalent counterions are present (as in refs 2–8). It is also shown that the solubilization capacity of the micelles depends strongly on the type and quantity of the counterions present in the solution. This observation is of practical importance, since it is directly related to the cleaning action of surfactant solutions.

The paper's organization is the following: section 2 contains the experimental methods, section 3 deals with the theoretical analysis and discussion of the results, and section 4 summarizes the concluding remarks.

2. Experimental Part

2.1. Materials and Sample Preparation. The surfactant used in the present work was SDP-2S (Empicol ESB70) from Wilson Co., with the formula $CH_3(CH_2)_{11}(OC_2H_4)_2OSO_3Na$. The ionic strength needed was achieved with NaCl and $AlCl_3 \cdot 6H_2O$ (Sigma) and/or $CaCl_2 \cdot 2H_2O$ (Aldrich). The contribution of cmc and ions, released from the micelles, on the ionic strength was neglected, for the salt and surfactant concentrations used. All the micellar solutions were prepared using deionized water (Milli-Q, Organex grade). The samples for light-scattering experiments were filtered twice with Millipore 100 and 220 nm filters before measurements in order to remove dust particles. The surfactant concentration used was 0.3 wt % (0.008 M) or less, which allowed us to avoid multiple light scattering. The solubilization experiments were performed with xylene (Sigma) and diisopropylbenzene (Merck) as the oil phase. The micelles were shaken in contact with the hydrocarbon for 4 h at 27 °C. The equilibrium solubilization was reached in about 2 h.

The light scattering experiments were done with Autosizer 4700C equipment (Malvern), supplied with an argon laser (Innova, Coherent), of 488 nm wavelength, and a K7032 CE 8-multibit 128-channel correlator. The solubilization capacity

* To whom correspondence should be addressed.
† Colgate-Palmolive Research and Development.
‡ Colgate-Palmolive Co.
® Abstract published in *Advance ACS Abstracts,* April 1, 1995.
(1) Israelachvili, J. N. *Intermolecular and Surface Forces*; Academic Press: London, 1991; Chapter 17.
(2) Mazer, N. A. In *Dynamic Light Scattering*; Pecora, R., Ed.; Plenum Press: London, 1985; Chapter 8.
(3) Mazer, N. A.; Benedek, G. B.; Carey, M. C. *J. Phys. Chem.* **1976**, *80*, 1075.
(4) Hayashi, S.; Ikeda, S. *J. Phys. Chem.* **1980**, *84*, 744.
(5) Missel, P. J.; Mazer, N. A.; Benedek, G. B.; Young, C. Y.; Carey, M. C. *J. Phys. Chem.* **1980**, *84*, 1044.
(6) Porte, G.; Appell, J.; Poggi, Y. *J. Phys. Chem.* **1980**, *84*, 3105.
(7) Van de Sande, W.; Persoons, A. *J. Phys. Chem.* **1985**, *89*, 404.
(8) Mishic, J. R.; Fisch, M. R. *J. Chem. Phys.* **1990**, *92*, 3222.
(9) Tanford, C. *The Hydrophobic Effect: Formation of Micelles and Biological Membranes*; Wiley: New York, 1980; Chapter 7.

measurements were performed by refractometry using Pulfrich refractometer PR2 (Carl Zeiss). The temperature in all measurements was maintained at 27 ± 0.1 °C.

2.2. Light Scattering Experiments. Measurements of the Diffusion Coefficients and Hydrodynamic Radii by Dynamic Light Scattering. The dynamic light-scattering (DLS) method detects the fluctuations in the scattered light intensity, or the intensity autocorrelation function[10]

$$g^{(2)}(\tau) = \frac{\langle E_S^*(t)\,E_S(t)\,E_S^*(t+\tau)\,E(t+\tau)\rangle}{\langle I^2 \rangle} \quad (2.1)$$

where E_S is the scattered electric field and I is the intensity of the scattered light. The intensity autocorrelation function $g^{(2)}(\tau)$ is related to the field autocorrelation function $g^{(1)}(\tau)$ by the expression

$$g^{(2)}(\tau) = 1 + |g^{(1)}(\tau)|^2 \quad (2.2)$$

According to the definition[10]

$$g^{(1)}(\tau) = \frac{\langle E_S^*(t+\tau)\,E_S(t)\rangle}{\langle I \rangle} \quad (2.3)$$

and is treated by means of cumulant expansion

$$\ln g^{(1)}(\tau) = \sum_n K_n \frac{(-\tau)^n}{n!} \quad (2.4)$$

where

$$K_n = (-1)^n \lim_{\tau \to 0} \frac{d^n}{d\tau^n} \ln g^{(1)}(\tau) \quad (2.5)$$

For systems of noninteracting particles[10]

$$K_1 = D_{SE}q^2 \qquad K_2 = K_3 = \ldots = 0 \quad (2.6)$$

where D_{SE} is the Stokes–Einstein diffusion coefficient[10,11]

$$D_{SE} = \frac{kT}{6\pi\eta R_h} \quad (2.7)$$

In eq 2.7 η is the solvent viscosity, R_h is the particle hydrodynamic radius, and kT is the thermal energy. Hence, by measuring the diffusion coefficient, one may determine the size of the particles. The described procedure defines the so-called z-average diffusion coefficient. However, in some cases this quantity showed slight dependence on the diaphragm or laser power used. For that reason in all further considerations we used the mass averaged values for the particle radii. These values were obtained by appropriate treatment of the measured z-average diffusion coefficients with the available Malvern software. The mass average radii obtained by this procedure were very close to those calculated directly from the z-average diffusion coefficient but were stable with respect to the laser power and diaphragm used.

In our case, however, we deal with nonspherical micelles (see ref 1 for more discussion on the micellar structures), which means that the measured hydrodynamic radius R_h represents an apparent quantity. Since the micelles are expected to have cylindrical shape with spherical caps (prolate spheroids)[1] we use expressions for the mobilities of cylinders derived by Brenner[12] (see also ref 13), viz.

$$f_{||} = \frac{8\pi\eta L}{r^2(2\beta + \alpha_{||})} \quad (2.8)$$

expresses the parallel mobility and

$$f_\perp = \frac{8\pi\eta L}{2r^2\beta + \alpha_\perp} \quad (2.9)$$

expresses the perpendicular mobility. L is the length of the cylinder, a is its radius assumed hereafter to be equal to that of the spherical micelles, formed by the same surfactant at lower concentrations of multivalent counterions at the same ionic strength, and r is the axis ratio ($r = L/2a$); also

$$\alpha_{||} = \frac{2}{(r^2 - 1)}(r^2\beta - 1) \quad (2.10)$$

$$\alpha_\perp = \frac{r^2}{(r^2 - 1)}(1 - \beta) \quad (2.11)$$

where

$$\beta = \frac{\cosh^{-1}(r)}{r(r^2 - 1)^{1/2}} \quad (2.12)$$

for $r > 1$ (prolate spheroids). The effective diffusion coefficient of a prolate spheroid can be written as a sum of parallel and perpendicular contributions

$$D = \frac{1}{3}(2D_\perp + D_{||}) \quad (2.13)$$

where

$$D_\perp = \frac{kT}{f_\perp} \qquad D_{||} = \frac{kT}{f_{||}} \quad (2.14)$$

Equating the Stokes–Einstein diffusion coefficient from 2.7 to that defined by 2.13, one obtains an equation for connecting the measured hydrodynamic radius R_h to some geometrical parameter of the prolate spheroid, e.g. the axis ratio, r. Some effects due to the presence of ionic atmosphere may affect the overall mobility of the micelle[13] but are neglected in the present consideration.

Determination of the Radius of Gyration by Measuring the Angular Dependence of the Scattered Light Intensity. The radii of gyration of polymer molecules could be obtained by using the Guinier–Fournet expression[14]

$$I(\theta) = I_0 \exp\left(\frac{-k(\theta)^2 R_g^2}{3}\right) \quad (2.15)$$

where I is the scattering intensity, θ is the scattering angle, R_g is the radius of gyration and $k(\theta)$ is the magnitude of the wave vector

$$k(\theta) = \frac{4\pi n}{\lambda} \sin\left(\frac{\theta}{2}\right) \quad (2.16)$$

n is the refractive index of the solution, and λ is the laser source wavelength (488 nm). By measuring the intensity of the scattered light at different angles and using eq 2.15, one obtains the value of the radius of gyration, R_g.

2.3. Determination of the Amount of Oil Solubilized in the Micelles. We measured the solubilization of oil into the micelles refractometrically following the approach developed by

(10) Pusey, P. N.; Tough, R. J. A. In *Dynamic Light Scattering*; Pecora, R., Ed.; Plenum Press: London, 1985; Chapter 2.
(11) Einstein, A. *Ann. Phys. (Leipzig)* **1905**, *17*, 549.
(12) Brenner, H. *Int. J. Multiphase Flow* **1974**, *1*, 195.

(13) Schumacher, G. A.; van de Ven, T. G. M. *J. Chem. Soc. Faraday Trans.* **1991**, *87*, 971.
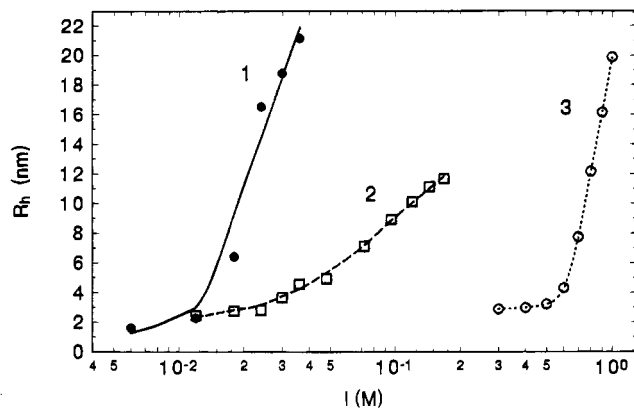(14) A. Guinier and G. Fornet, *Small Angle Scattering of X-Rays*, Wiley: New York, 1955.

Figure 1. Apparent hydrodynamic radius (R_h) vs ionic strength of the solution (I) for different salts: curve 1, AlCl$_3$; curve 2, CaCl$_2$; and curve 3, NaCl. The surfactant concentration is 0.008 M.

Yurzhenko.[15] This method has been successfully applied for studying the solubilization of hydrocarbons into anionic micelles.[16-18] It is based on the fact that the refractive index of the surfactant solution usually increases with the solubilized amount of hydrocarbon and reaches a plateau for the case of saturation. It was shown that[15]

$$V_t \frac{n_t^2 - 1}{n_t^2 + 2} = V_s \frac{n_s^2 - 1}{n_s^2 + 2} + V_h \frac{n_h^2 - 1}{n_h^2 + 2} \quad (2.17)$$

where the subscripts t, s, and h are related to the total system, surfactant solution, and hydrocarbon respectively, V is the partial volume, and n is the refractive index. Assuming ideal mixing,

$$V_t = V_s + V_h \quad (2.18)$$

After simple transformations, one obtains

$$V_h = V_s \frac{\beta_s - \beta_t}{\beta_s - \beta_h} \quad (2.19)$$

where

$$\beta_i = \frac{n_i^2 - 1}{n_i^2 + 2}, \quad i = t, s, h \quad (2.20)$$

Equation 2.19 allows calculation of the amount of hydrocarbon in the surfactant solution, if V_s, n_t, n_s and n_h are known.

3. Results and Discussion

Most of the results presented and discussed in this section are mainly for anionic (SDP-2S) micelles in the presence of trivalent (Al^{3+}) counterions, because the effects are more pronounced in comparison with divalent ones. Still, some results with divalent (Ca^{2+}) ions are also reported and discussed.

3.1. Hydrodynamic and Gyration Radii, Shape, and Aggregation Numbers of the Micelles. Figure 1 shows the apparent micellar hydrodynamic radius (R_h) as a function of the ionic strength of the solution I. The latter was obtained using different salts, AlCl$_3$ (curve 1), CaCl$_2$ (curve 2), and NaCl (curve 3), and a constant surfactant concentration or 0.008 M. It is evident that above a certain value of the ionic strength the micelles
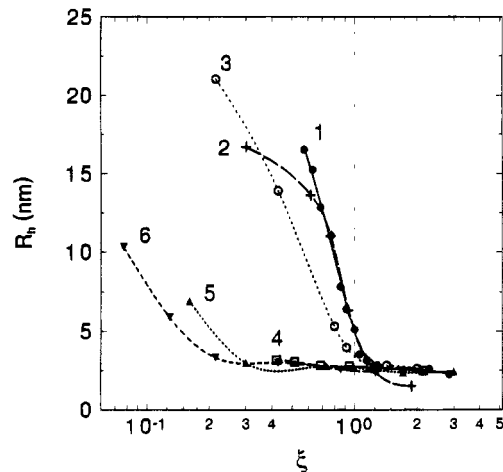
(15) Yurzhenko, A. J. *Zh. Obshch. Khim.* **1946**, *16*, 1171.
(16) Markina, N.; Pospelova, K. A.; Rebinder, P. A. *Kolloid Zh.* **1954**, *16*, 366.
(17) Mitina, T. D.; Korshuk, E. F.; Aleksandrovich, Kh. M. *Kolloid Zh.* **1977**, *39*, 983.
(18) Panicheva, L. P.; Tretyakov, N. Y. *Kolloid Zh.* **1990**, *52*, 590.

Figure 2. Apparent hydrodynamic radius (R_h) vs ξ. Curve 1 corresponds to ionic strength 0.024 M, a constant amount of surfactant, $C_t = 0.008$ M, and a variable concentration of Al. Curve 2 is for the same ionic strength, a variable concentration of surfactant, and a constant amount of Al^{3+} (0.003 M). Curve 3 corresponds to variation of the Al^{3+} ions at ionic strength 0.064 M and $C_t = 0.004$ M. Curve 4 is equivalent to curve 1, but the metal counterion in this case is Ca^{2+}. Curves 5 and 6 are obtained again by varying the amount of Ca^{2+} at ionic strength 0.064 M and 0.128, respectively.

undergo transition from roughly spherical to cylindrical shape (detected as an increase of the measured hydrodynamic radius). These values of the ionic strengths, however, are different for the different salts used, i.e. different counterions present. For NaCl (curve 3) the shape transition occurs between 0.5 and 0.6 M, which is in agreement with the result for sodium dodecyl sulfate obtained by other authors.[2-9] For the case of CaCl$_2$ (curve 2) the shape transition takes place at a much lower ionic strength, between 0.024 and 0.03 M. The effect is even stronger when trivalent counterions such as Al^{3+} are present. The transition value of the ionic strength is between 0.012 and 0.018 M. These results confirm that the type (i.e. the valence) of counterion is important for the micellar structure, as we already discussed above.

The dependence of the apparent hydrodynamic radius (R_h) measured by DLS (see the previous section) on the ratio of the surfactant amount *in micellar form* and the amount of dissolved counterions is shown in Figure 2. The ionic strength was constant, adjusted with NaCl when necessary. The points are experimentally determined while the curves present least square fits. The solid curve 1 was obtained by varying the concentration of the trivalent counterions and keeping the total surfactant concentration, C_t, constant (0.008 M). The decrease of the concentration of trivalent ions leads to an increase in $\xi = (C_t - \text{cmc})/z C_M$ (C_M is the multivalent ions concentration, C_t is the total surfactant concentration, and z is the valence of the respective counterion: 3 for the case of Al and 2 for the case of Ca). The ionic strength in this case was also maintained constant (0.024 M), by adjusting it with the appropriate amount of NaCl for each experimental point. It is seen that the apparent hydrodynamic radius exhibits a sharp change for $\xi \approx 1$, i.e. when there is one trivalent ion per three surfactant molecules incorporated in the micelles. The finding is confirmed by the data on the dashed curve 2 in Figure 2. The latter was obtained by varying the total surfactant concentration (C_t) while the amount of trivalent counterions and ionic strength (0.024 M) were kept constant. The agreement between the two curves is very good and suggests that the ratio of the surfactant in micellar form and trivalent

counterions, ξ, is indeed an important parameter, determining the micellar size and shape (see below). Some discrepancy is observed in the left parts of curves 1 and 2. Most probably it is due to the fact that the micellar size depends on the total surfactant concentration (at given ξ; see below) and decreases with the dilution. Above we have assumed that the critical micellization concentration (cmc) does not depend on the amount of trivalent counterions present in the solution at constant ionic strength. This assumption is justified since cmc depends mostly on the total ionic strength and rather weakly on the specific type of the dissolved microions,[9] which was also confirmed by our own light scattering experiments. For ionic strength equal to 0.024 M, we obtained cmc (SDP-2S) = 1.33×10^{-4} M. The cmc is rather low; hence, even if some variance is present, it should not affect the result significantly. The dotted curve 3 in Figure 2 is for higher ionic strength (0.064 M) maintained by using AlCl$_3$ and NaCl. The cmc in this case is 7.8×10^{-5} M. The surfactant concentration in this case was 0.004 M in order to be able to reach lower values of the ratio ξ. It can be seen that the slope of the curve around $\xi = 1$ is less than it is in the case of lower ionic strength. The reason is that the monovalent counterions compete more actively with the trivalent ones in binding to the micellar surface and the changes in the micellar shape are slightly suppressed. On the other hand, this higher ionic strength allows us to reach lower values of the ratio ξ, which yields greater sizes (first point from the left).

The situation with divalent counterions (Ca^{2+} in our experiments) is different. The increase in the apparent hydrodynamic radius is less pronounced. Curve 4 was obtained at the same ionic strength (0.024 M) as curve 1, but in the presence of calcium ions instead of aluminium ions. The surfactant concentration was 0.008 M as for curve 1. One sees that the micellar size in this case does not change at $\xi = 1$ ($z = 2$) as when aluminium ions are present. This is evidence for the lower impact of divalent ions on the micellar shape and size which may be due to the greater competition of monovalent ions with divalent ions as compared with trivalent ones. If the concentration of calcium ions increases, the micellar size also increases; see curve 5, which corresponds to ionic strength 0.064 M and surfactant concentration 0.004 M (cf. curve 2; the slopes of the two curves differ strongly). However, the jump in the micellar size does not take place at $\xi = 1$ as in the case of aluminium (see curves 1–3) but at values of ξ between 0.2 and 0.3. Hence, the amount of calcium ions that provides a change in the micellar size is greater than the amount which would be necessary for the neutralization of the micellar surface ionic groups. Curves 5 and 6 are for ionic strengths equal to 0.064 and 0.128 M, respectively. The change in the micellar radius is greater but takes place approximately at the same value of ξ.

Figure 3 illustrates the dependence of the apparent hydrodynamic radius, obtained by using the measured values for diffusion coefficient and eq 2.7, on the surfactant concentration *at constant* ξ and ionic strength 0.024 M. The right points of each curve are plotted on curve 1 in Figure 2. The dilution of the samples is performed carefully in order to keep ξ constant. In this case the micellar radius increases with the surfactant concentration.

In principle the dependence of the apparent hydrodynamic radius on the concentration of micelles can be attributed also to the manifestation of intermicellar interactions[2] and is linear for moderate surfactant concentrations. When monovalent electrolyte is present in the solution, it is known that the micelles do not exhibit
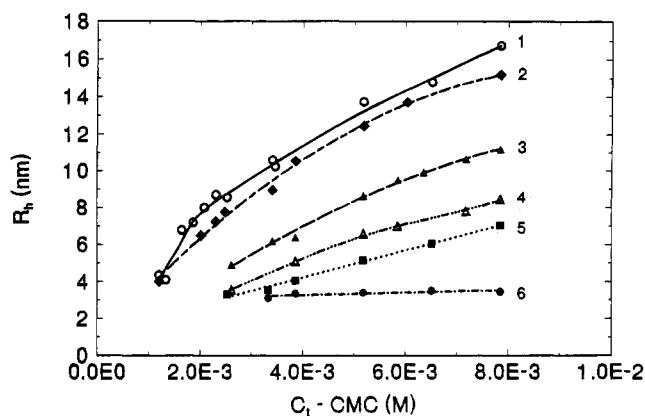

Figure 3. Dependence of the apparent hydrodynamic radius (R_h) on the surfactant concentration (C_t−cmc) in the presence of Al^{3+} counterions and ionic strength 0.024 M. ξ is constant for each curve and corresponds to 0.67, curve 1; 0.73, curve 2; 0.77, curve 3; 1.00, curve 4; 1.07, curve 5; 1.23, curve 6.

sphere to rod transition below 0.5 M concentration of electrolyte[2-8,19] (see also Figure 1). Chang and Kaler[19] reported a nonlinear dependence of the apparent micellar hydrodynamic radius for sodium dodecyl sulfate in the presence of monovalent electrolyte, NaCl, for very high ionic strengths (0.6 and 0.8 M). As they assumed, such a dependence of the apparent micellar hydrodynamic radius on the surfactant concentration for cylindrical micelles (see curves 1–4 in Figure 3) can be interpreted as a change in their aggregation number. Hence, we may conclude that the aggregation number (i.e. the size) of the cylindrically shaped micelles increases with the total surfactant concentration. This is illustrated in Figure 3, where the measured hydrodynamic radius (in the presence of Al^{3+}) is plotted as a function of the total surfactant concentration. In our case, when multivalent counterions are present, this is achieved at much lower ionic strengths (0.024 M in presence of AlCl$_3$ and 0.128 M in presence of CaCl$_2$) in comparison with the similar systems when monovalent counterions are present[19] (0.6 - 0.8 M NaCl). Each curve is obtained at constant ratio ξ, starting from 0.67 (curve 1) up to 1.23 (curve 6). It is also seen that for lower values of ξ (e.g. below 1, high concentration of Al^{3+}) the hydrodynamic radii exhibit nonlinear increase with the surfactant concentration, while for greater values (above 1, which means low concentration of Al^{3+} and spherical micelles) the increase is almost linear; see curves 5 and 6 in Figure 3. The linear increase of the apparent hydrodynamic radius with the concentration of surfactant indicates the presence of attractive intermicellar interactions which interferes with determination of the aggregation number, based on changes of observed hydrodynamic radius. Such attraction is probably due to the appearance of ionic correlation forces between the double layers of the micelles.[20] The observed intermicellar attraction is not very strong since the slope of the lines (curves 5 and 6 in Figure 3) is moderate and will be neglected in the present consideration. Detailed analysis of the importance of the ionic correlation forces between micelles in the presence of multivalent ions will be presented elsewhere. In the case of divalent ions such as Ca^{2+} (Figure 4) the increase of the apparent hydrodynamic radius with the surfactant concentration is almost linear for both cases ($\xi = 0.09$, curve 1, and $\xi = 1$, curve 2) and the effect of the actual change of the micellar size can hardly be separated from that due to the attractive interactions. The ionic strength in this case was 0.128 M.

(19) Chang, N. J.; Kaler, E. W. *J. Phys. Chem.* **1985**, *89*, 2996.
(20) Kralchevsky, P. A.; Paunov, V. P. *Colloids Surf.* **1992**, *64*, 245.
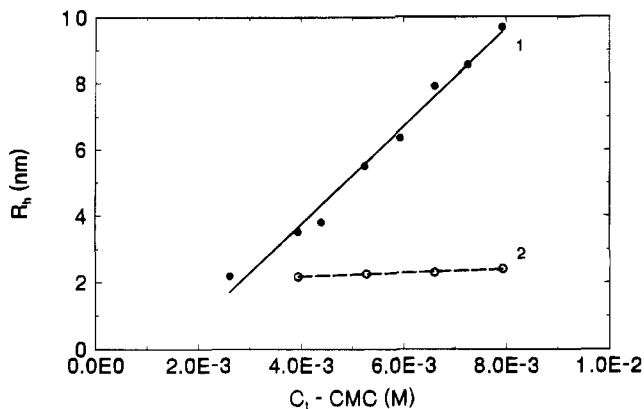
Figure 4. Dependence of the apparent hydrodynamic radius (R_h) on the surfactant concentration (C_t–cmc) in the presence of Ca^{2+} counterions and ionic strength 0.128. ξ is constant for each curve and corresponds to 0.09, curve 1; and 1.00, curve 2.

The increase of the micellar radius with the total amount of surfactant present in the solution (i.e. curves, similar to those shown in Figures 3 and 4), but in the presence of monovalent counterions, is successfully explained by the theory of Missel et al.[2-8,19] However, in our case (multivalent counterions) this theory predicts weaker change of the measured hydrodynamic radius with the surfactant concentration than the one experimentally observed. The discrepancy between the theoretical model and the experimental results is more obvious if we compare the theoretical expression for the micellar aggregation number as a function of the surfactant concentration[2,5]

$$N = N_0 + 2[K(X - X_{cmc})]^{1/2} \qquad (3.1)$$

where N is the aggregation number of the cylindrical micelle, N_0 is the same quantity for spherical micelles, K is constant, depending on the chemical potential of the surfactant monomers in spherical and cylindrical packing, and X and X_{cmc} are the molar fractions of surfactant in the solution and critical micelization concentration, respectively. Equation 3.1 predicts a linear dependence of the micellar aggregation number if plotted vs $(X - X_{cmc})^{1/2}$ with an intercept equal to the aggregation number of a spherical micelle. Since the aggregation numbers of the micelles cannot be obtained directly by means of static light scattering measurements (Zimm plot cannot be used when a change of particles size or aggregation number takes place), we had to calculate them. For that reason we needed the geometrical parameters of the micelles. The assumption of micellar cylindrical shape allowed us to use the expressions for diffusion coefficient of non-spherical particles (eqs 2.13 and 2.14) in order to treat the experimental data for micellar diffusion coefficients. The geometrical parameters of cylindrical micelles are included in the expressions for the mobilities of cylinders. Thus by using eqs 2.8–2.14 we can calculate the length of the rodlike micelles. By using the calculated values and some literature data[1,9] for the length of the hydrophobic tail (1.672 nm), volume of the hydrophobic tail (0.3502 nm³), and the length of the polyoxyethylene plus polar head groups (1.1 nm), one can obtain the volume of the hydrophobic core. Dividing the volume of the cylindrical oil core by the volume of a single hydrophobic chain, one can obtain the respective aggregation numbers. In Figure 5 some typical experimental results for the aggregation number of micelles in the presence of Al^{3+} ions are shown. They are determined as described above. Curves 1–4 in Figure 5 (obtained by least square fits) correspond to ξ = 0.67, 0.73, 1.07, and 1.23, respectively (cf. curves 1, 2, 5,
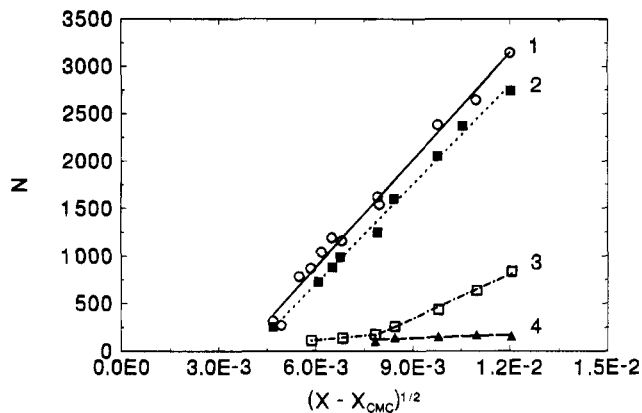

Figure 5. Micellar aggregation number (N) vs the micellar molar fraction ($X - X_{cmc}$) at ionic strength 0.024 M: curve 1, ξ = 0.67; curve 2, 0.73; curve 3, 1.07; and curve 4, 1.23.
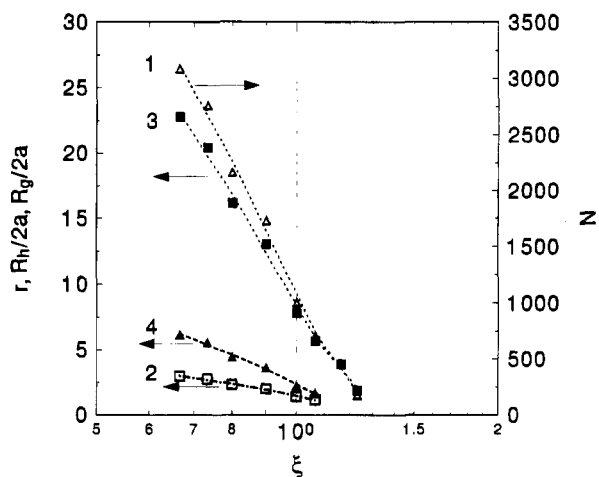

Figure 6. Micellar aggregation number (N) (curve 1), apparent hydrodynamic radius (R_h) (curve 2), length of the micellar cylinder over its diameter (r) (curve 3), and radius of gyration (R_g) (curve 4) vs ξ. All solutions are in presence of Al^{3+} counterions.

and 6 in Figure 3). One sees that the plots for ratios equal to 0.67 and 0.73 (line 1 and 2) are linear, but the intercepts in both cases are negative, which has no physical meaning (the aggregation number is always positive value). In the case ξ = 1.07 (curve 3), one can distinguish two linear regions with different slopes. The first three points from the left in curve 3 can be extrapolated to give an intercept corresponding roughly to the aggregation number of a spherical micelle (56 in this case[1]). The whole curve, however, cannot be explained in the framework of the model based on eq 3.1. One may speculate that some change in the micellar structure takes place at the point where the two linear portions of the curve meet, but such option is not included in the model of Missel et al.[2,5] The last line 4 can be extrapolated to aggregation numbers close to that for spherical micelles, similarly to the linear portion with smaller slope of curve 3. Since the amount of Al^{3+} ions decreases from curve 1 to 4, we may conclude that at high concentrations of trivalent ions and surfactant (higher ξ), the available theory fails to explain the experimental data. Another reason for such discrepancy (beside the possible structural changes) is the presence of intermicellar interactions which are not included in the model.

Figure 6 shows the micellar aggregation number (N), calculated as described above (curve 1), the hydrodynamic micellar radius (R_h), measured by dynamic light scattering (curve 2, see section 2.2), the ratio of the length over the diameter of the cylindrical micelle ($r = L/2a$) calculated
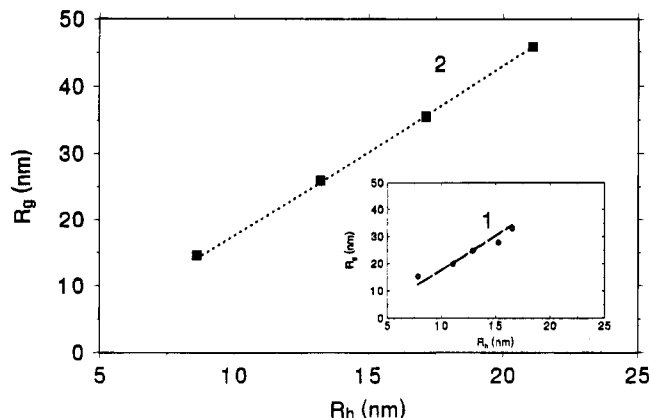
Figure 7. Radius of gyration (R_g) as a function of the apparent hydrodynamic radius (R_h) in the presence of Al^{3+} counterions. The points correspond to the experimental measurements for ionic strength 0.064 M (■) and 0.024 M (○). The lines (1 for 0.024 and 2 for 0.064 M) follow eq 3.2. The surfactant concentration is 0.008 M.

from the experimentally obtained hydrodynamic radius (curve 3, see eqs 2.7–2.14), and the radius of gyration (R_g), (curve 4) which was determined experimentally with the help of the relationship 2.15. The solution contains 0.008 M SDP-2S and a mixture of NaCl and $AlCl_3$ to maintain the total ionic strength at 0.024 M. All the quantities decrease as ξ approaches 1 (cf. Figure 2). When ξ is below 1, there is a big difference between the experimental values of R_h and R_g. The latter is an indication for the existence of nonspherical objects (rodlike micelles). This is confirmed by curve 3, which represents the length over the diameter of the cylindrical micelles r as a function of ξ. The greater ξ is, the smaller r is. r approaches 1 in the case of spherical micelles. Figure 7 shows the relation between the radius of gyration (R_g) and the apparent hydrodynamic radius (R_h) for micelles in SDP-2S solution (in the presence of Al^{3+} ions) with 0.008 M surfactant concentration and ionic strengths of 0.024 M (curve 1) and 0.064 M (curve 2). The value of ξ was varied from 0.67 to 1 (curve 1) and from 0.25 to 0.67 (curve 2). The two radii are measured independently by means of the procedures described above while the lines correspond to the theoretical expression[8,21]

$$R_g^2 = L^2\left\{\frac{l_p}{3L} - \frac{l_p^2}{L^2} + \frac{2l_p^4}{L^4}\left[\frac{L}{l_p} - 1 + \exp\left(-\frac{L}{l_p}\right)\right]\right\} + \frac{a^2}{2}$$

(3.2)

where l_p is the persistent length, which is used as an adjustable parameter. The values obtained are $l_p = 190$ nm and $l_p = 165$ nm for curves 1 and 2, respectively. It is seen that the theoretical expression 3.2 is in very good agreement with the experimental results, especially for the higher ionic strength 0.064 M. This fact confirms indirectly the assumption that the micelles have a cylindrical shape. For rigid rods $l_p / L \to \infty$ and

$$R_g^2 = \frac{L}{12} + \frac{a^2}{2}$$

(3.3)

while for random coils $l_p / L \to 0$ and

$$R_g^2 = \frac{L l_p}{3}$$

(3.4)

(see ref 8). The persistent length is an indication whether the micellar rods may bend spontaneously in the solution due to thermal fluctuations. It is related to the bending
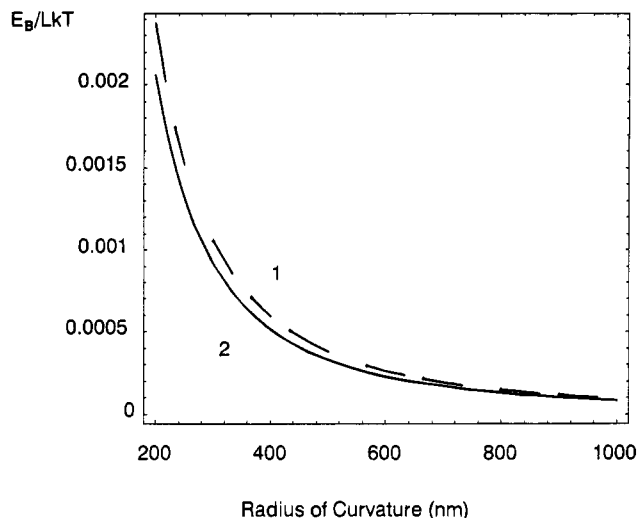

Radius of Curvature (nm)

Figure 8. Bending energy of rod-shaped micelles vs radius of curvature. The dashed curve 1 corresponds to ionic strength 0.024 M ($l_p = 190$ nm) and the solid curve 2 to 0.064 M ($l_p = 165$ nm). The surfactant concentration is 0.008 M.

energy of the cylindrical rod by means of the relationship[6–8,21,22]

$$E_B = kT\frac{L l_p}{2R_c^2}$$

(3.5)

The quantity R_c in eq 3.5 denotes the curvature radius of the micellar rods. The diameter of the rod is neglected in comparison with its length when deriving eq 3.5, which in some cases is a rather strong approximation. Despite of these simplifications[21] we use eq 3.5 for estimations of the bending energy of cylindrical micelles, E_B, as a function of the radius of curvature (R_c). The results for the bending energy per unit length of cylindrical SDP-2S micelles (with total surfactant concentration equal to 0.008 M) in the presence of Al^{3+} ions are shown in Figure 8. The ionic strengths were 0.024 M (curve 1) and 0.064 M (curve 2). It is seen that, for radii of curvature above 200 nm, the bending of the micelles due to thermal fluctuations is rather probable (the bending energy is below $0.003kT$). Also, at the lower ionic strength, 0.024 M, the micellar rods seem to be slightly harder than at the higher one, 0.064 M. The latter conclusion is not surprising, but the effect is at the threshold of the experimental accuracy.

3.2. Solubilization Properties of SDP-2S Micelles in the Presence of Multivalent Counterions. Figure 9 shows the hydrodynamic radii of empty micelles (curve 1) and oil-containing micelles (curve 2) and the volume of the solubilized oil divided by the solution volume (curve 3) as functions of ξ. The surfactant concentration and ionic composition for all the curves are the same as for curve 1 in Figure 2 (in fact curve 1 in Figure 2 is identical with curve 1 in Figure 9). The comparison between the sizes of empty and oil-containing micelles shows that for $\xi < 1$ the oil-containing micelles are smaller than the empty ones while for $\xi > 1$ they are larger. A possible reason is that the cylindrical aggregates become unstable when filled with oil and disassemble into smaller ones. A similar observation was made by Bayer et al.[23] for cationic surfactants in the presence of organic additives and NaCl.

(21) Yamakawa, H. *Modern Theory of Polymer Solutions*; Harper and Row: New York, 1971.

(22) Landau, L. D.; Lifshitz, E. M. *Statistical Physics*; Pergamon Press: London, 1977; Chapter 12.

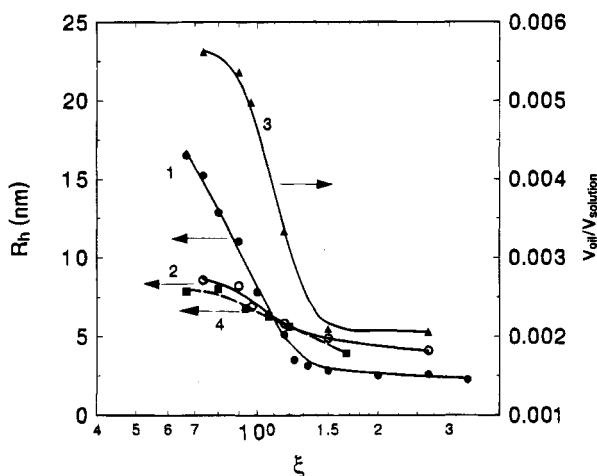(23) Bayer, O.; Hoffmann, H.; Ulbricht, W.; Thurn, H. *Adv. Colloid Interface Sci.* **1986**, *26, 177.*

Figure 9. Apparent hydrodynamic radius (R_h) of empty micelles (curve 1), oil-containing micelles in presence of xylene (curve 2), solubilized amount of xylene (curve 3), and oil-containing micelles in the presence of diisoprpylbenzene (curve 4) as a function of ξ. The parameters are the same as for curve 1 in Figure 2.
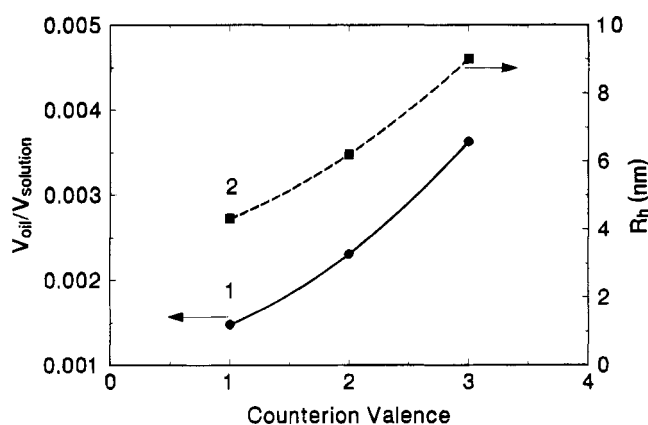

Figure 10. Variation of the solubilizing capacity of the surfactant solution and apparent hydrodynamic radius (R_h) of solubilized micelles vs the counterion valence. The ions used were Na^+, Ca^{2+}, and Al^{3+}. The ionic strength was 0.024 M.

In the other region, $\xi > 1$, where the micelles are roughly spherical, the oil leads to swelling of the surfactant aggregates, probably without changing their aggregation number, which leads to an increase in their size. The different lines denoting the experimental results for oil-containing micelles (curves 2 and 4) are for two types of oil phases: xylene and diisopropylbenzene. It can be concluded that the two hydrocarbons lead to identical increase in the particle size and hence exhibit identical solubilization. Curve 3 presents the change of the solubilized quantity of hydrocarbon (xylene) as a function of ξ. The presence of trivalent ions plays a significant role also for the solubilization performance of the system. The greater the concentration of Al^{3+} ions, the greater the solubilization. The difference in the amount solubilized oil is almost 3 times if we compare the respective values in the left ($\xi < 1$) and the right ($\xi > 1$) sides of curve 3.

A possible explanation of the enhanced solubilization capacity of the surfactants in the presence of multivalent ions is that the latter decrease the repulsion between the polar head groups of the surfactant molecules in the micelles and thus increase the micellar radius. This concept is confirmed also by Figure 10. It illustrates the

variation of the solubilizing capacity of the micellar solution with the valence of the counterions present in the bulk (the ionic strength is 0.024 M). It is seen that the amount of solubilized oil (curve 1) increases from mono- to divalent and further to trivalent ions in accordance with the increase of the micellar size (curve 2). This dependence was checked with different types of multi-valent counterions (Ca, Mg, Al, Fe) and the agreement between the obtained results was very good.

Another observation was that the polydispersity of the aggregates decreased with the solubilization. Thus the typical polydispersity for empty micelles was between 28 and 30% while after solubilization it became (reproducibly) about 20–24%. A possible explanation of this fact, as discussed above, is that the empty cylindrical micelles could grow easily in longitudinal direction, providing larger polydispersity. However, after filling with oil they acquire a more globular shape, determined by the balance of different thermodynamic factors, and may become more monodisperse.

4. Concluding Remarks

In the present study we examined the size and shape of SDP-2S micelles in the presence of multivalent ions. It was shown that the multivalent ions can lead to transition from sphere to cylinder at ionic strengths much lower than those necessary to induce such shape change with monovalent electrolyte. This effect is particularly pronounced for trivalent counterions such as Al^{3+}. It seems questionable whether the Al^{3+} ions are present in trivalent form (as assumed in the present work) or as different complexes, e.g. with OH^- groups. Our estimations based on the stability of the various complexes,[24] $Al(OH)^{2+}$ and $Al(OH)_2^+$, showed that, for the concentrations of $AlCl_3$ we used, the trivalent form is prevalent (above 90%). Besides, one may speculate that the complexes of Al^{3+} and OH^-, although present in the bulk, may be destroyed when reaching the micellar surface. The cylindrical shape of the larger micelles has been established by measuring the angular dependence of the scattered light. In addition the persistent lengths for some rod-shaped micelles were obtained and the energy of bending of such rods were estimated. These estimations showed that the bending of such micelles, caused by thermal fluctuations, is rather probable. The solubilization capacity of SDP-2S was shown to be also dependent on the presence of divalent and trivalent ions. It was found that the solubilization capacity increases when varying the counterion valence from 1 to 3. The analysis of the solubilization of oil into cylindrical micelles suggests that the surfactant aggregates disassemble due to the penetration of oil in the hydrophobic core. The established increase of the solubilization capacity of anionic surfactants in the presence of divalent and furthermore trivalent counterions could be of practical importance since it is directly related to the cleaning action of detergent compositions.

(24) Bonchev, P. *Introduction in Analytical Chemistry*; Nauka i Iz-kustvo: Sofia, 1985 (in Bulgarian).